A theoretical study of two-magnon light scattering in triangular antiferromagnets on a plane

1994 J. Phys.: Condens. Matter 6 7763

(http://iopscience.iop.org/0953-8984/6/38/014)

J. Phys.: Condens. Matter 6 (1994) 7763–7771. Printed in the UK

A theoretical study of two-magnon light scattering in triangular antiferromagnets on a plane

Y Watabe, T Suzuki and Y Natsume

Department of Physics, Faculty of Science, Chiba University, Yayoi-cho, Inage-ku, Chiba 263, Japan

Received 5 November 1993, in final form 24 May 1994

Abstract. Two-magnon Raman scattering in triangular Heisenberg antiferromagnets on a two-dimensional plane is discussed on the basis of the 120° structure, where spins are confined on the plane by the single-ion-type anisotropy, by the use of the exchange–scattering mechanism. Spectra obtained by calculation reflect the symmetric properties of the present non-collinear spin structure. In addition to the normal structure in spectra of the α mode which is symmetric with respect to space inversion, we can find anomalous structure of β and γ modes which lacks symmetry with respect to space inversion. The former appears at twice the excitation energy for the single mode, which is also found in collinear structures for two-sublattice Néel states. In contrast, the latter is caused by the following anomaly characterizing the present 120° structure in the triangular lattice antiferromagnets: the magnon for the β mode with wave-number vector $+k$ is effectively coupled with that for the γ mode with $+k$.

1. Introduction

Recently, much attention has been paid to the magnetic properties in triangular antiferromagnetic systems with Heisenberg-type exchange interaction in connection with the problem of how such properties differ from those of antiferromagnetic systems on a square lattice. In a square lattice, the collinear Néel structure is believed to be the ground state on the two-sublattice structure, though quantum fluctuation plays an important role. On the other hand, we are faced with the problem of the relation between the non-collinear Néel structure (120° structure) and the frustration essentially contained within the system, if we discuss magnetic properties of an antiferromagnetic system on a triangular lattice. Such a problem can be discussed in the context of the characteristic properties of the symmetry. These characteristic features can appear in optical spectra, which are due to excitations of antiferromagnetic magnons on this lattice. Among optical spectra for antiferromagnetic magnons, the Raman scattering is well confirmed [1, 2, 3] to be essential for investigations of properties in antiferromagnetic compounds. In short, excitations of two magnons at k and $-k$ for each mode appear in Raman spectra of the collinear state in the two-sublattice structure [4].

The purpose of the present study is to develop a theory of the scattering of light by spin systems in triangular antiferromagnets through the use of spin-dependent electronic polarizability. In short, we apply the theory of exchange scattering in antiferromagnets investigated by Moriya [1] and Fleury *et al* [2, 3] to the calculation of Raman spectra in triangular antiferromagnets assuming that the ground state is the 120° Néel structure on the plane.

0953-8984/94/387763+09$19.50

In brief, we clarify the appearance of magnon modes which lack inversion symmetry, as well as that for modes with inversion symmetry. Further, we point out characteristic features in Raman spectra for two-magnon scattering which are caused by these properties of the symmetry, showing results of numerical calculation. In addition, the comparison of the present calculation with experimental work on VCl_2 [5] and $LiCrO_2$ [6] is discussed.

2. Magnon dispersion of the system

The Hamiltonian on a plane discussed here is

$$\mathcal{H} = J \sum_{\langle l,m,n \rangle} (S_{Al} \cdot S_{Bm} + S_{Bm} \cdot S_{Cn} + S_{Cn} \cdot S_{Al}) + D \sum_i \left\{ \left(S^z_{Ai}\right)^2 + \left(S^z_{Bi}\right)^2 + \left(S^z_{Ci}\right)^2 \right\} \tag{1}$$

where A, B and C denote the three sublattices. Here, the first term (J) represents the Heisenberg-type antiferromagnetic exchange interaction for nearest neighbours and the second term (D) the single-ion-type anisotropic interaction for each spin. Because of the assumption that D is not negative, spins are confined on the c-plane (xy-plane) by this anisotropy. The symmetry of the present system is D_{6h} (the space group is $P6/mmm$). The ground state of this antiferromagnetic system is well confirmed to be the 120° Néel structure as in previous work [7]. This state is schematically shown in figure 1(a). Figure 1(b) shows primitive vectors for both the magnetic unit cell and the chemical unit cell. Here, indices 1–6 are defined as the nearest-neighbour sites for a site 0.

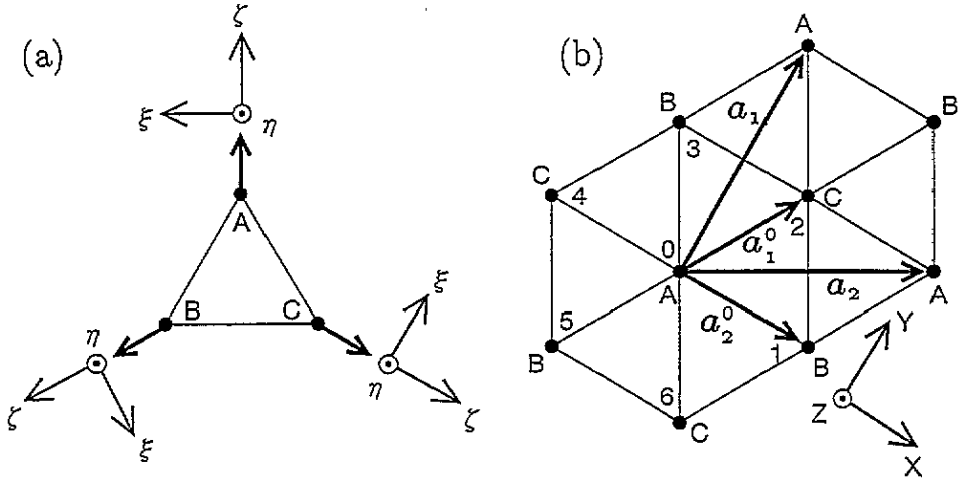

Figure 1. (a) The 120° Néel structure on the three-sublattice structure A, B, C. The local coordinate for each site is shown by (ξ, η, ζ). (b) The primitive vectors for the magnetic unit cell forming a three-sublattice structure are shown by a_1 and a_2. Those for the chemical unit cell are also shown by a_1^0 and a_2^0. Nearest-neighbour sites for a site 0 are denoted by 1, 2, ... 6.

For this system in the case of $D \geqslant 0$, the magnon dispersion expressed as linear Holstein–Primakoff spin waves has been obtained by Oguchi [8], by the use of Bogoliubov transformation. Furthermore, such a dispersion can also be derived [8, 9] by the method of the helical spin wave structure. The obtained dispersions for magnons are expressed as follows:

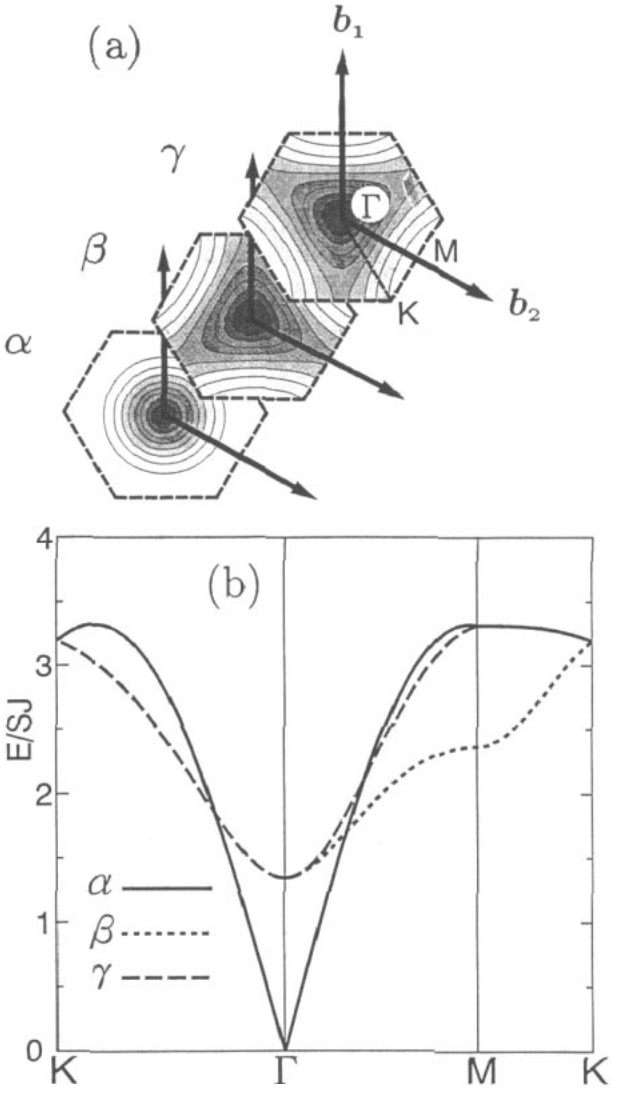

Figure 2. (a) The first Brillouin zone for the magnetic unit cell. A vertex and lateral of this hexagon are denoted by K and M, respectively. The primitive vectors of the reciprocal lattice are shown by b_1 and b_2. Dispersions of magnons, α, β and γ modes, are illustrated for $D/J = 0$ by shading; lighter shade indicates higher energy. (b) The dispersion of magnons α, β and γ on the lines of K–Γ–M–K for $D/J = 0.2$. On the line of K–Γ, β and γ modes coincide. In contrast, α and γ modes coincide on the line of M–K. The α mode is the Goldstone mode.

$$E_\alpha(\boldsymbol{k}) = SJ\epsilon_{\boldsymbol{k}}(0) \qquad E_\beta(\boldsymbol{k}) = SJ\epsilon_{\boldsymbol{k}}(2\pi/3) \qquad E_\gamma(\boldsymbol{k}) = SJ\epsilon_{\boldsymbol{k}}(4\pi/3) \tag{2}$$

where

$$\epsilon_{\boldsymbol{k}}(\theta) = \sqrt{\{3 - \Phi_{\boldsymbol{k}}(\theta)\}\{3 + 2\Phi_{\boldsymbol{k}}(\theta) + 2D/J\}}. \tag{3}$$

Here,

$$\Phi_k(\theta) = \cos\{(k_1 + k_2)/3 + \theta\} + \cos\{(k_1 - 2k_2)/3 + \theta\} + \cos\{(-2k_1 + k_2)/3 + \theta\}. \quad (4)$$

In these expressions, the wave-number vector k in the first magnetic Brillouin zone is expressed by k_1 and k_2 in the region of $-\pi \leqslant k_1, k_2 \leqslant \pi$ as

$$k = k_1 b_1 + k_2 b_2 \quad (5)$$

where the reciprocal lattice vectors b_1 and b_2 are shown in figure 2(a).

Such a dispersion for magnons is also shown in the first Brillouin zone in figure 2(a) and figure 2(b). It should be noted that modes for β and γ are invariant for the rotation of $2\pi/3$, lacking symmetry with respect to space inversion, though the α mode is symmetric with respect to space inversion. Namely, the β mode at $-k$ corresponds to the γ mode at $+k$. In other words, we obtain the γ mode if we rotate the β mode by $\pi/3$. Furthermore, as shown in figure 3, we can expect the following behaviour of spins S_A, S_B and S_C for $(D/J) \ll 1$ in the limit of $k \to 0$. In the α mode, three spins rotate on the c-plane maintaining the 120° structure. It is quite natural that the α mode is the *Goldstone mode*. In contrast to this, for β and γ modes, vibrations of spins expand out of the c-plane destroying the 120° structure. (We would like to point out that movements of spins are gradually restricted on the c-plane with increasing D/J on the basis of our numerical study.)

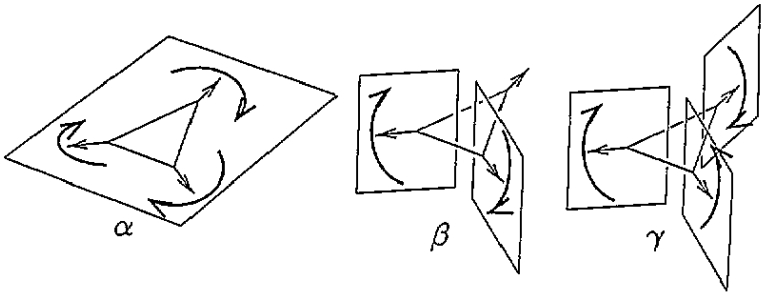

Figure 3. Movements of spins are schematically shown for magnons of α, β and γ modes for $(D/J) \ll 1$ in the limit of $k \to 0$. It is easily seen that the α mode is the Goldstone mode.

3. Raman scattering by magnons

We consider the spin-dependent polarizability: in particular, the polarizability associated with a pair of ionic spins according to the method of Moriya [1]. In fact, the polarizability is described as

$$\alpha_Q^{(\omega_0)} = \frac{1}{V} \sum_{j,l} \alpha_{j,l}^{(\omega_0)} \exp(-iQ \cdot R_j) \quad (6)$$

in which Q is the difference of wave-number vectors between incident and scattered light. In the long-wavelength approximation, we define Q to be zero. In consideration of the nearest-neighbour exchange coupling for a j site, $\alpha_{j,l}^{(\omega_0)}$ is written by the following tensor $P_{j,j+d}$ for each nearest neighbour d:

$$\alpha_{j,j+d}^{(\omega_0)} = P_{j,j+d}\ (S_j \cdot S_{j+d}). \quad (7)$$

Nearest-neighbour sites 1–6 for a site 0 are shown in figure 1(b). The tensor $P_{j,j+d}$ can be determined by the local symmetry. Under the condition that we consider the single plane

on which the triangular lattice lies, components for xz, zx, yz and zy vanish, because the system shows mirror symmetry for the c-plane. Therefore, we concentrate on the behaviour of $\alpha^{(\omega_0)}_{j,j+d}$ on the c-plane. Consequently, the following forms are obtained for tensors $P_{j,j+d}$:

$$\sum_d P_{j,j+d}(\boldsymbol{S}_j \cdot \boldsymbol{S}_{j+d}) = \begin{bmatrix} p_1 & 0 \\ 0 & p_2 \end{bmatrix} (\boldsymbol{S}_j \cdot \boldsymbol{S}_{j+1} + \boldsymbol{S}_j \cdot \boldsymbol{S}_{j+4}) + \frac{1}{4}\begin{bmatrix} p_1 + 3p_2 & -\sqrt{3}(p_1 - p_2) \\ -\sqrt{3}(p_1 - p_2) & 3p_1 + p_2 \end{bmatrix} (\boldsymbol{S}_j \cdot \boldsymbol{S}_{j+2} + \boldsymbol{S}_j \cdot \boldsymbol{S}_{j+5}) + \frac{1}{4}\begin{bmatrix} p_1 + 3p_2 & \sqrt{3}(p_1 - p_2) \\ \sqrt{3}(p_1 - p_2) & 3p_1 + p_2 \end{bmatrix} (\boldsymbol{S}_j \cdot \boldsymbol{S}_{j+3} + \boldsymbol{S}_j \cdot \boldsymbol{S}_{j+6}). \tag{8}$$

This equation for the polarizability can be rewritten as follows in terms of irreducible expressions A_{1g} (z^2), E_{2g} ($x^2 - y^2$) and E_{2g} (xy):

$$\sum_d P_{j,j+d}(\boldsymbol{S}_j \cdot \boldsymbol{S}_{j+d}) \equiv \begin{bmatrix} p_{xx} & p_{xy} \\ p_{yx} & p_{yy} \end{bmatrix} = \begin{bmatrix} p_+ & 0 \\ 0 & p_+ \end{bmatrix} \sum_{d=1}^{6} \boldsymbol{S}_j \cdot \boldsymbol{S}_{j+d} + \begin{bmatrix} p_- & 0 \\ 0 & -p_- \end{bmatrix} \frac{1}{\sqrt{6}} (2\boldsymbol{S}_j \cdot \boldsymbol{S}_{j+1} + 2\boldsymbol{S}_j \cdot \boldsymbol{S}_{j+4} - \boldsymbol{S}_j \cdot \boldsymbol{S}_{j+2} - \boldsymbol{S}_j \cdot \boldsymbol{S}_{j+3} - \boldsymbol{S}_j \cdot \boldsymbol{S}_{j+5} - \boldsymbol{S}_j \cdot \boldsymbol{S}_{j+6}) + \begin{bmatrix} 0 & p_- \\ p_- & 0 \end{bmatrix} \frac{1}{\sqrt{2}} (\boldsymbol{S}_j \cdot \boldsymbol{S}_{j+2} - \boldsymbol{S}_j \cdot \boldsymbol{S}_{j+3} + \boldsymbol{S}_j \cdot \boldsymbol{S}_{j+5} - \boldsymbol{S}_j \cdot \boldsymbol{S}_{j+6}) \tag{9}$$

where $p_+ = \frac{1}{2}(p_1 + p_2)$, while $p_- = (\sqrt{6}/4)(p_1 - p_2)$. In the general consideration of the symmetry for the Raman spectrum, only A_{1g} and E_{2g} modes can be active in this D_{6h} system. The base of A_{1g} is proportional to z^2 (the corresponding polarizability is $p_{xx} + p_{yy} \sim p_+$ and p_{zz}), while those for E_{2g} are proportional to $x^2 - y^2$ (the corresponding polarizability is $p_{xx} - p_{yy} \sim p_-$) and xy (the polarizability is $p_{xy} \sim p_-$). Therefore, the polarizability should be expressed with respect to such bases.

The scattered cross section of the scattered light ω for the incident light ω_0 is expressed in the following form of Fourier transformation for time τ:

$$\frac{\mathrm{d}^2\sigma}{\mathrm{d}\Omega\,\mathrm{d}\omega} = \frac{V^2}{(4\pi)^2}\frac{\omega_0\omega^3}{c^4}\frac{1}{2\pi}\int_{-\infty}^{\infty} \mathrm{d}\tau \exp\{\mathrm{i}(\omega - \omega_0)\tau\}\langle e_0 \alpha_0^{(\omega_0)}(0)(1 - \tilde{n}\cdot\tilde{n})\alpha_0^{(\omega_0)}(\tau)e_0\rangle \tag{10}$$

where the bracket $\langle\,\rangle$ indicates the thermal average for the temperature T;

$$\langle G\rangle = \frac{\mathrm{Tr}[G\,\exp(-\mathcal{H}/k_\mathrm{B}T)]}{\mathrm{Tr}[\exp(-\mathcal{H}/k_\mathrm{B}T)]}. \tag{11}$$

Here, e_0 is the unit vector for the polarization of the incident light and $\tilde{n}$ the unit vector pointing to the scattered direction. Furthermore, the subscript $\mathbf{0}$ of α means the long-wavelength approximation for the light, i.e., $\pm\boldsymbol{Q} \to \mathbf{0}$, and $\alpha_0^{(\omega_0)}(\tau)$ denotes the time variation due to the Hamiltonian (1) of the system in the following manner:

$$\alpha_0^{(\omega_0)}(\tau) = \exp(-\mathrm{i}\mathcal{H}\tau/\hbar)\,\alpha_0^{(\omega_0)}\exp(\mathrm{i}\mathcal{H}\tau/\hbar). \tag{12}$$

In equation (10), $\tilde{n}\cdot\tilde{n}$ represents diadics. It should be noted that the expression of the A_{1g} mode commutes with the Heisenberg Hamiltonian in equation (1) in the case of $D = 0$. This implies that the contribution to the Raman scattering by this mode is zero for $D = 0$ or quite small even for $D \neq 0$. Thus, we concentrate on the contribution of the E_{2g} mode hereafter.

Next, we express each pair of spins by magnon operators α, β and γ derived before. Among these magnon operator terms, quadratic terms contribute to the inelastic scattering process. In fact, we obtain the following expression for the scattering cross sections of equation (10) in experimental configurations xx and xy (yx) for Raman spectra ($\omega \neq \omega_0$) taking into account the fact that excitations for $E_\beta(k) + E_\beta(-k)$ by light corresponds to those for $E_\beta(k) + E_\gamma(k)$ and that those for $E_\gamma(k) + E_\gamma(-k)$ can be replaced by those for $E_\gamma(k) + E_\beta(k)$:

$$\left[\frac{d^2\sigma}{d\Omega\, d\omega}\right]_{xx} = \frac{S^2}{(4\pi)^2}\frac{\omega_0\omega^3}{c^4}\sum_k \big[2\{W_{1k}(0)\}^2\,[\{1+n_\alpha(k)\}^2\delta(\omega-\omega_0+2E_\alpha(k)/\hbar) + \{n_\alpha(k)\}^2\delta(\omega-\omega_0-2E_\alpha(k)/\hbar)] + \{W_{1k}(2\pi/3)+W_{1k}(4\pi/3)\}^2 \times[\{1+n_\beta(k)\}\{1+n_\gamma(k)\}\delta(\omega-\omega_0+(E_\beta(k)+E_\gamma(k))/\hbar) + \{n_\beta(k)\}\{n_\gamma(k)\}\delta(\omega-\omega_0-(E_\beta(k)+E_\gamma(k))/\hbar)]\big] \tag{13}$$

$$\left[\frac{d^2\sigma}{d\Omega\, d\omega}\right]_{xy} = \frac{S^2}{(4\pi)^2}\frac{\omega_0\omega^3}{c^4}\sum_k \big[2\{W_{2k}(0)\}^2\,[\{1+n_\alpha(k)\}^2\delta(\omega-\omega_0+2E_\alpha(k)/\hbar) + \{n_\alpha(k)\}^2\delta(\omega-\omega_0-2E_\alpha(k)/\hbar)] + \{W_{2k}(2\pi/3)+W_{2k}(4\pi/3)\}^2 \times[\{1+n_\beta(k)\}\{1+n_\gamma(k)\}\delta(\omega-\omega_0+(E_\beta(k)+E_\gamma(k))/\hbar) + \{n_\beta(k)\}\{n_\gamma(k)\}\delta(\omega-\omega_0-(E_\beta(k)+E_\gamma(k))/\hbar)]\big] \tag{14}$$

where $n(k)$ denote Bose–Einstein distribution functions, and $W_{1k}(\theta)$ and $W_{2k}(\theta)$ are described as follows:

$$W_{1k}(\theta) = p_+\frac{1}{2}\frac{D}{J}\frac{3-\Phi_k(\theta)}{\epsilon_k(\theta)} - p_-\frac{1}{2}\left(\frac{9}{2}+\frac{D}{J}\right)\frac{\Delta_{1k}(\theta)}{\epsilon_k(\theta)} \tag{15}$$

$$W_{2k}(\theta) = p_-\frac{1}{2}\left(\frac{9}{2}+\frac{D}{J}\right)\frac{\Delta_{2k}(\theta)}{\epsilon_k(\theta)}. \tag{16}$$

In equation (15), $\Phi_k(\theta)$ is given in equation (4). In these expressions for $W_{1k}(\theta)$ and $W_{2k}(\theta)$, the denominators denote the magnon dispersion presented in equation (3). On the other hand, $\Delta_{1k}(\theta)$ and $\Delta_{2k}(\theta)$ in the numerators represent polarization patterns corresponding to symmetries of Raman-active modes $E_{2g}(x^2-y^2)$ and $E_{2g}(xy)$, respectively:

$$\Delta_{1k}(\theta) = \frac{1}{\sqrt{6}}[-\cos\{(k_1+k_2)/3+\theta\} - \cos\{(k_1-2k_2)/3+\theta\} + 2\cos\{(-2k_1+k_2)/3+\theta\}] \tag{17}$$

$$\Delta_{2k}(\theta) = \frac{1}{\sqrt{2}}[-\cos\{(k_1+k_2)/3+\theta\} + \cos\{(k_1-2k_2)/3+\theta\}]. \tag{18}$$

Raman spectra are theoretically reproduced by expressions (13)–(18). Here, it should be noted that spectra for β and γ modes reflect the *joint density of states* between β and γ modes, i.e. $\sum_k \delta(\omega-\omega_0 \pm (E_\beta(k)+E_\gamma(k))/\hbar)$, while those for the α mode are formed principally by the density of states for the α mode.

4. Numerical results and discussion

Spectra obtained by numerical calculations are shown in figure 4 and figure 5 for the xx configuration of the E_{2g} $(x^2 - y^2)$ component. Figure 4 shows Stokes scattering for $D/J = 0.0$, 0.2 and 0.5 at $T = 0$, in which the broad low-energy peak and the sharp high-energy one are clearly found. In order to investigate the origin of these structures, we show the calculated spectrum for each mode for $D/J = 0.2$ in figure 5. For the α mode, the magnons at $+k$ and $-k$ form the structure for $2E_\alpha(k)$. This scattering yields the sharp peak at $6.6SJ$. On the other hand, the unusual properties of β and γ modes discussed before exhibit characteristic features in the two-magnon spectra. In fact, the magnon for the β mode at $+k$ is effectively coupled with that for the γ mode at $+k$ in the calculated spectra. Such characteristic features can be seen as the peak structure with broad shoulders around 5.7 and $6.3SJ$. That is, the peak at $5.7SJ$ originates from M points which form saddle points on the dispersion of magnons, as shown in figure 2. That is, β and γ modes have values of $2.4SJ$ and $3.3SJ$, respectively, at M points. In addition, the broad convex shoulder is produced dominantly by the joint density of states between β and γ modes which extend to K points from M points.

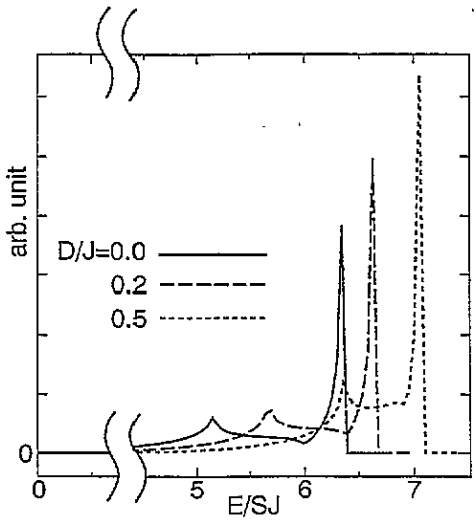

Figure 4. The calculated Stokes scattering in Raman spectra in the xx configuration for the E_{2g} $(x^2 - y^2)$ symmetry at $T = 0$. The values of D/J are 0, 0.2 and 0.5.

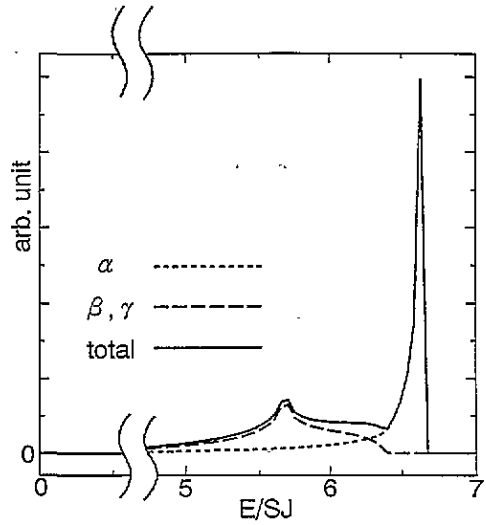

Figure 5. The spectrum of two magnons for only the α mode is shown by the dotted curve. The dashed curve shows the spectrum of magnons effectively coupled with β and γ modes. The value of $D/J = 0.2$. The spectrum considering all modes shown in figure 4 is illustrated by the solid curve. In the region of $E \geqslant 6.4SJ$, dotted and solid curves coincide.

We would like to emphasize that characteristic features for the joint density of states between β and γ modes originate from the properties of the 120° structure on the plane in the triangular lattice. The detailed behaviour of the broad convex shoulder is dependent on values of D/J.

Finally, we would like to mention the comparison of our calculation with experimental work on Raman scattering for magnetic excitations in VCl_2 [5] and $LiCrO_2$ [6], though a

system whose ground state is the 120° structure on the c-plane has not yet been reported.

Compounds VX_2 (X=Cl, Br) have the typical triangular structure with Heisenberg antiferromagnetic interaction. Nevertheless, the Néel structure for these compounds VX_2 is well confirmed to be a 120° structure on the ac-plane because of the single-ion-type axial anisotropy with respect to the c-axis expressed as $-D\sum_i \left(S_i^z\right)^2$. While magnon dispersion of corresponding α, β and γ modes for this structure with axial anisotropy can be calculated numerically [10, 11], the two-magnon Raman spectra cannot be obtained, because we cannot yet perform the Bogoliubov transformation of spin waves. As a result of numerical calculation [10, 11], we find that any mode is symmetric with respect to space inversion. (Namely, it is easily shown that any mode is invariant for $\pi/3$ rotation, in connection with the trigonal symmetry D_{3h} of the three-sublattice structure on the triangular lattice.) Thus, two-magnon spectra for $E_\alpha(k) + E_\alpha(-k)$, $E_\beta(k) + E_\beta(-k)$ and $E_\gamma(k) + E_\gamma(-k)$ are expected to show the conventional structure [4] which is lacking from the characteristic broad structure discussed here. Namely, the present calculation cannot be applied to the analysis of Raman spectra in VX_2. The qualitative discussion has already been presented [5] without considering the single-ion-type anisotropy (i.e., $D = 0$).

On the other hand, the present 120° structure on the c-plane is one of the candidates for the ground state of $LiCrO_2$ [12]. In fact, the magnetic scattering is observed [6] around 360 cm^{-1} in the Raman spectra, which corresponds to $13.3J$ by the use of the reported value $J = 39$ K [13]. However, the calculated sharp peak at $19J$ and the broad convex shoulder around $15J$ in spectra for $D = 0$ are not in agreement with such an observation. Thus, we would like to point out that candidates [12] other than the 120° structure on the c-plane should be adopted for the ground state of $LiCrO_2$.

Here, we would like to discuss the honeycomb lattice. Though it has D_{6h} symmetry, the well known collinear Néel state appears because of the two-sublattice structure. It is easily shown [11] that two-magnon modes are degenerate and symmetric with respect to space inversion. As a result, we obtain the conventional structure in Raman spectra for twice the magnon excitation, which is well confirmed [4] in collinear states.

Quite recently, the spin structure of $AgCrO_2$ has been discussed by Oohara *et al* [14] on the basis of magnetic-susceptibility measurements and neutron-diffraction study. They have pointed out that the long-range order is suppressed, though it has the possibility of forming a compound with the 120° structure on the c-plane. Experimental work on optical spectra in $AgCrO_2$ has not yet reported. The behaviour of magnetic scattering in this compound has not yet been studied. Such experimental work is strongly desirable.

In summary, the problem of finding compounds whose ground state is the 120° structure on a c-plane has not yet been solved. Therefore, the comparison between remarkable properties of Raman scattering in the present theoretical calculation and experimental results, and the investigation on the effect of magnon–magnon interactions [15] in Raman spectra for this kind of antiferromagnetic system on such characteristic lattices are subjects for future study.

Acknowledgments

Thanks are due to Professor N Suzuki of Osaka University and Dr T Nakayama of Chiba University for valuable discussions.

References

[1] Moriya T 1967 *J. Phys. Soc. Japan* **23** 490; 1968 *J. Appl. Phys.* **39** 1042
[2] Fleury P A, Porto S P and Loudon R 1967 *Phys. Rev. Lett.* **18** 658
[3] Fleury P A and Loudon R 1968 *Phys. Rev.* **166** 514
[4] For example,
Cottam M G and Lockwood D J 1986 *Light Scattering in Magnetic Solids* (New York: Wiley)
[5] Sugawara K and Yamada I 1993 *J. Phys.: Condens. Matter* **5** 1427
[6] Suzuki M, Yamada I, Kadowaki H and Takei F 1993 *J. Phys.: Condens. Matter* **5** 4225
[7] Mekata M 1986 *Butsuri* **41** 968 (in Japanese)
[8] Oguchi T 1983 *J. Phys. Soc. Japan Suppl.* **52** 183
[9] Shiba H private communication
[10] Suzuki T and Natsume Y 1987 *J. Phys. Soc. Japan* **56** 1577
In this reference, α, β and γ modes correspond to E_-, E_0 and E_+ modes respectively.
[11] Watabe Y 1994 unpublished
[12] Soubeyroux J L, Fruchart D, Marmeggi J C, Fitzgerald W J, Delmas C and Le Flem G 1981 *Phys. Status Solidi* a **67** 633
[13] Delmas C, Le Flem G, Fouassier C and Hagenmuller P 1978 *J. Phys. Chem. Solids* **39** 55
[14] Oohara Y, Mitsuda S, Yoshizawa H, Yamaguchi N, Kurihara H, Asano T and Makata M 1994 *J. Phys. Soc. Japan* **63** 847
[15] Elliott R J and Thorpe M F 1969 *J. Phys. C: Solid State Phys.* **2** 1630